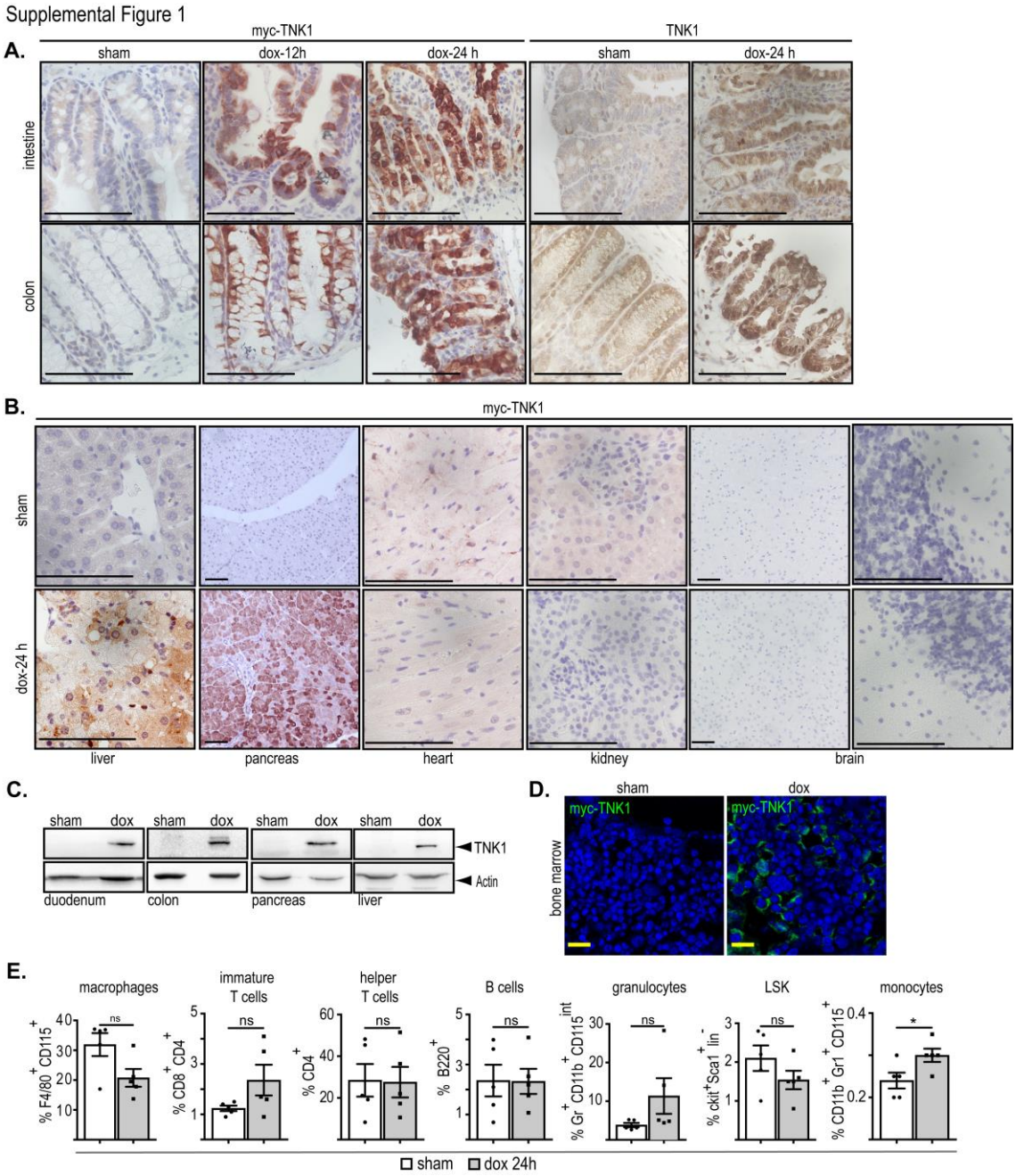

Supplemental Figure 1. (A) Twenty-four hours after doxycycline administration mice express TNK1 in the small and large intestine. Representative images display staining directed against Myc-tagged-TNK1 and TNK1. Both, Myc-tagged-TNK1 and TNK1 staining show TNK1 expression along crypts in the gut. TNK1 expression is not detectable in control mice. **(B)** Twenty-four hours after doxycycline challenge, TNK1 expression is detectable besides gut, also in pancreas and liver. TNK1 is not expressed in other vital organ such as heart, brain or kidney. **(C)** Western-blot shows expression of TNK1 in various tissue 24h after doxycycline challenge (n=3). **(D)** Illustrative IF images show Myc-TNK1 expression in bone marrow of the TNK1-expressing mice. **(E)** Hematopoietic composition of the bone marrow is not affected by TNK1 expression. The bar graphs depict quantified flow cytometric data (n=5/group). Data are expressed as the mean ± SEM. Differences were tested by parametric two-tailed, unpaired Student's t-tests (*p≤0.05, **p<0.001, ***p<0. 0001). Scale bar 100µm.

Supplemental Figure 2

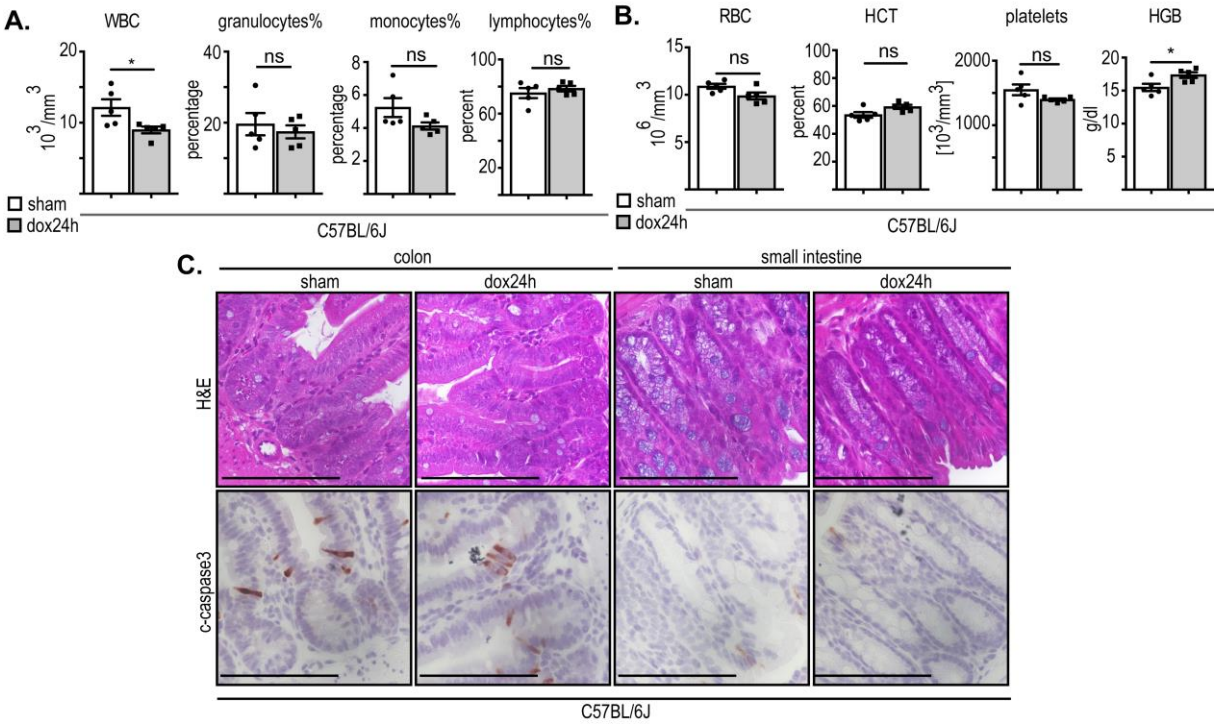

Supplemental Figure 2. Doxycycline dosing and administration does not contribute to the systemic pathological effect observed upon TNK1 expression. Effect of doxycycline dosing and administration was examined in C57BL/6J mice exposed to saline or doxycycline (50ug/g i.p.) for 24hours. **(A, B)** Graphs represent comparable haematological blood parameters of the mice treated with saline or doxycycline. **(C)** Illustrative images show normal and comparable intestinal architecture of the C57BL/6J mice upon doxycycline or saline administration. Data are expressed as the mean ± SEM. Differences were tested by parametric two-tailed, unpaired Student's t-tests (*p≤0.05, **p<0.001, ***p<0. 0001). Scale bar 100µm.

Supplemental Figure 3

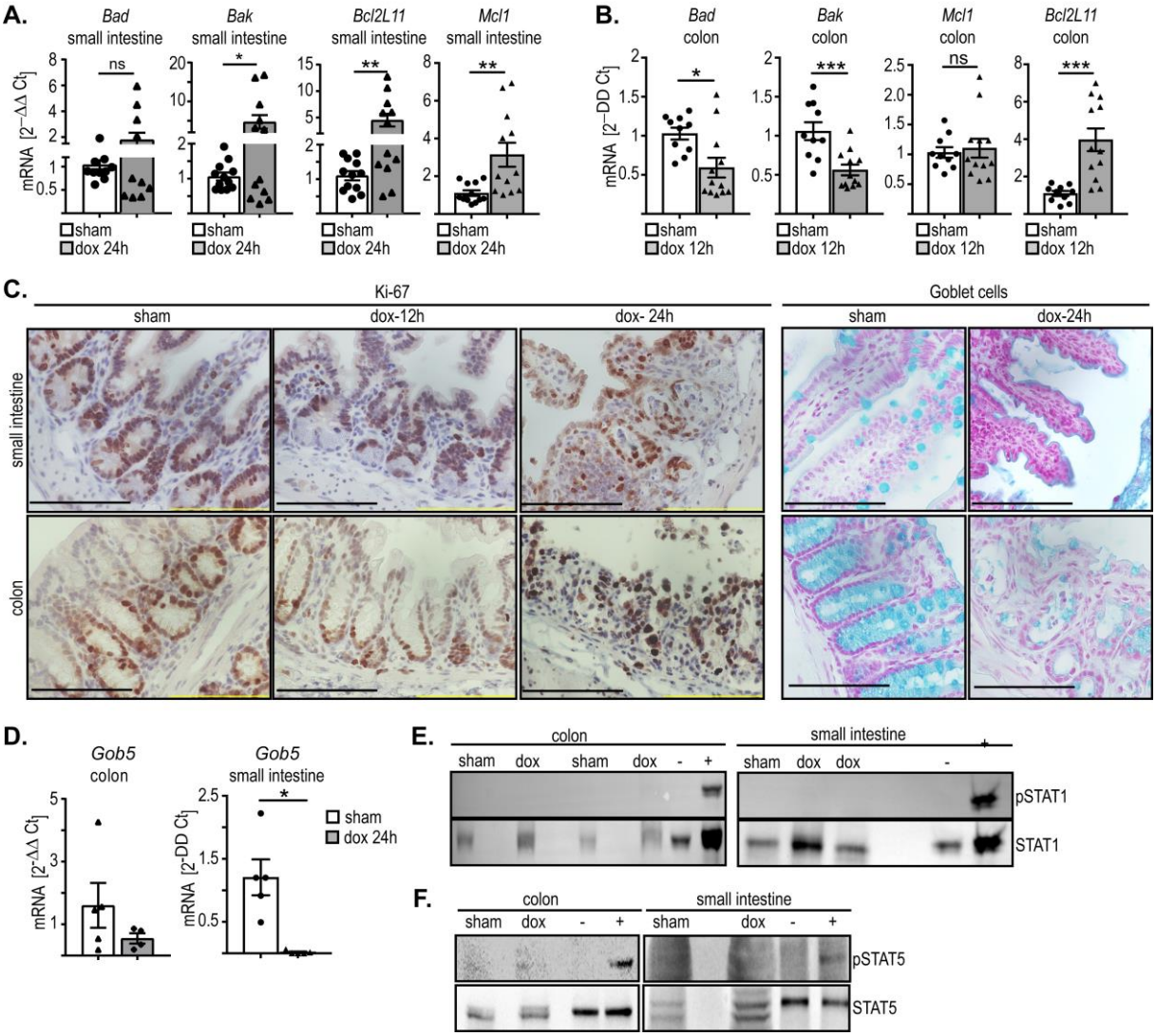

Supplemental Figure 3. (A) Graphs display changes in mRNA levels of pro-apoptotic (*Bad*, *Bak*, and *Bcl2l11*) and pro-survival (*Mcl2*) members of the Bcl2 family in small intestine and colon 24h after induced TNK1 expression (n=10/group). **(B)** TNK1-expressing mice exhibit decreased expression of pro-apoptotic genes *Bad* and *Bak* and upregulated expression of *Bcl2L11* (*Bim*) in colon 12h after dox administration. Expression of pro-survival gene *Mcl1* in the colon is not changed in response to TNK1 expression (n=10/group). **(C, left panels)** Representative images of Ki67 staining show progressive loss of viable proliferative crypts in the small and large intestine of TNK1-expressing mice, 12h and 24h after doxycycline exposure. **(C, right panels)** Alcian blue stained small and large intestine sections display distortion of the crypt architecture, formation of crypt abscess with the loss of goblet cells in TNK1-expressing mice, 24h after doxycycline challenge. **(D)** Graphs represent mRNA levels of goblet cell marker *Gob5* in the small and large intestine (n=5/group) **(E, F)** STAT1 and STAT5 are not phosphorylated/activated as result of the TNK1 expression in the small and large intestine 24h upon TNK1 expression. Representative Western blots display expression of both STAT1 and STAT5 and lack of their phosphorylation (n=3). Data are expressed as the mean ± SEM. Differences were tested by parametric two-tailed, unpaired Student's t-tests (*p≤0.05, **p<0.001, ***p<0. 0001). Scale Bar: 100µm.

Supplemental Figure 4

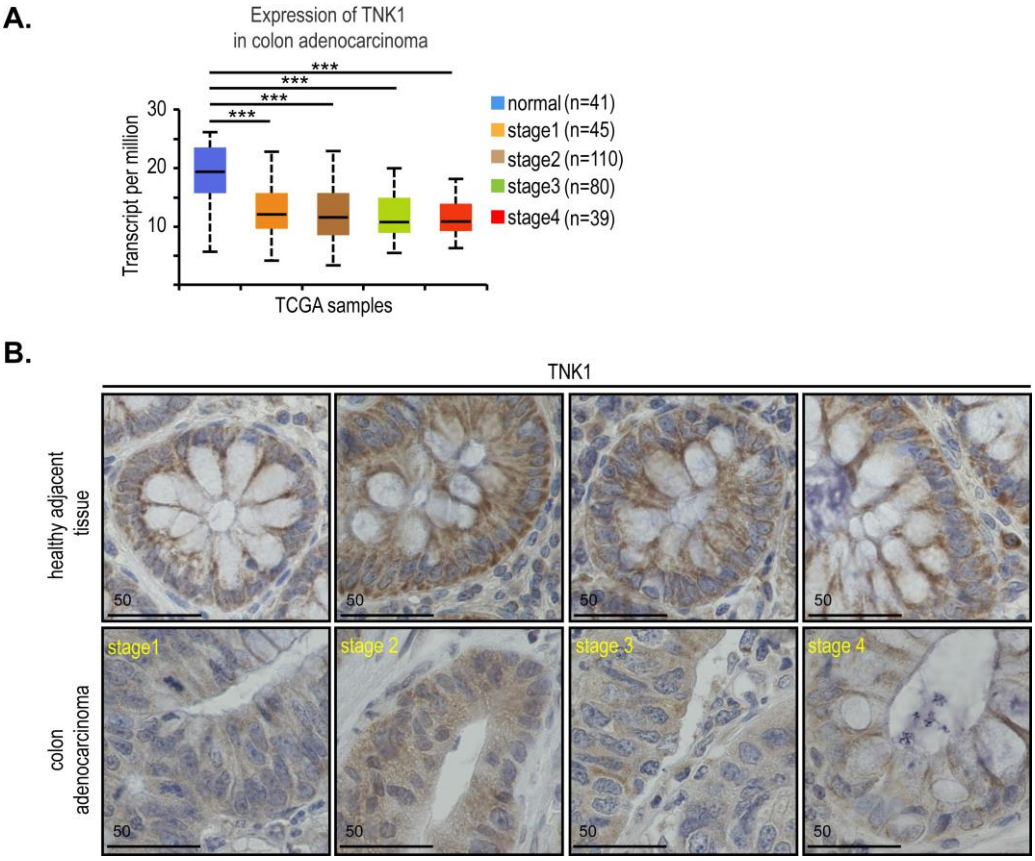

Supplemental Figure 4. **(A)** Box-plots depict relative *Tnk1* expression in normal and subgroups of colon adenocarcinoma samples (data are obtained from interactive web resource UALCAN for analysing cancer transcriptome data (1). Number of samples is indicated in the legend **(B)** Immunostaining against TNK1 illustrates the expression of TNK1 or its absence on the protein level in epithelial cells in healthy colon tissue and colon adenocarcinoma.

Supplemental Figure 5

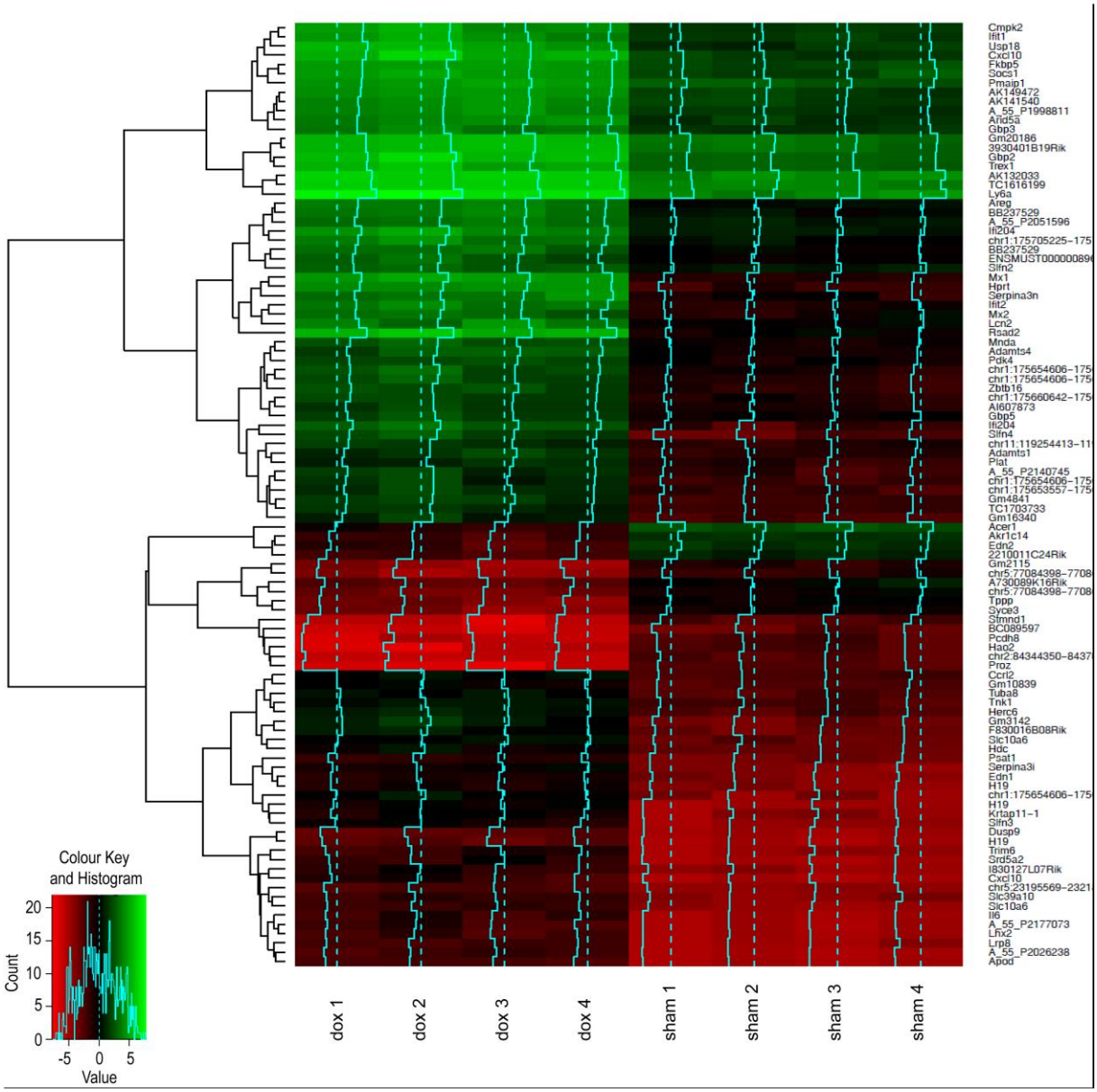

Supplemental Figure S5. Heat map shows differentially expressed genes in the control (sham (0,9%NaCl)) and TNK1-expressing mice (dox). Each group consisted of four samples. Gene expression profiles are shown in rows. Green indicates upregulated genes, whereas red the opposite.

Supplemental Figure 6

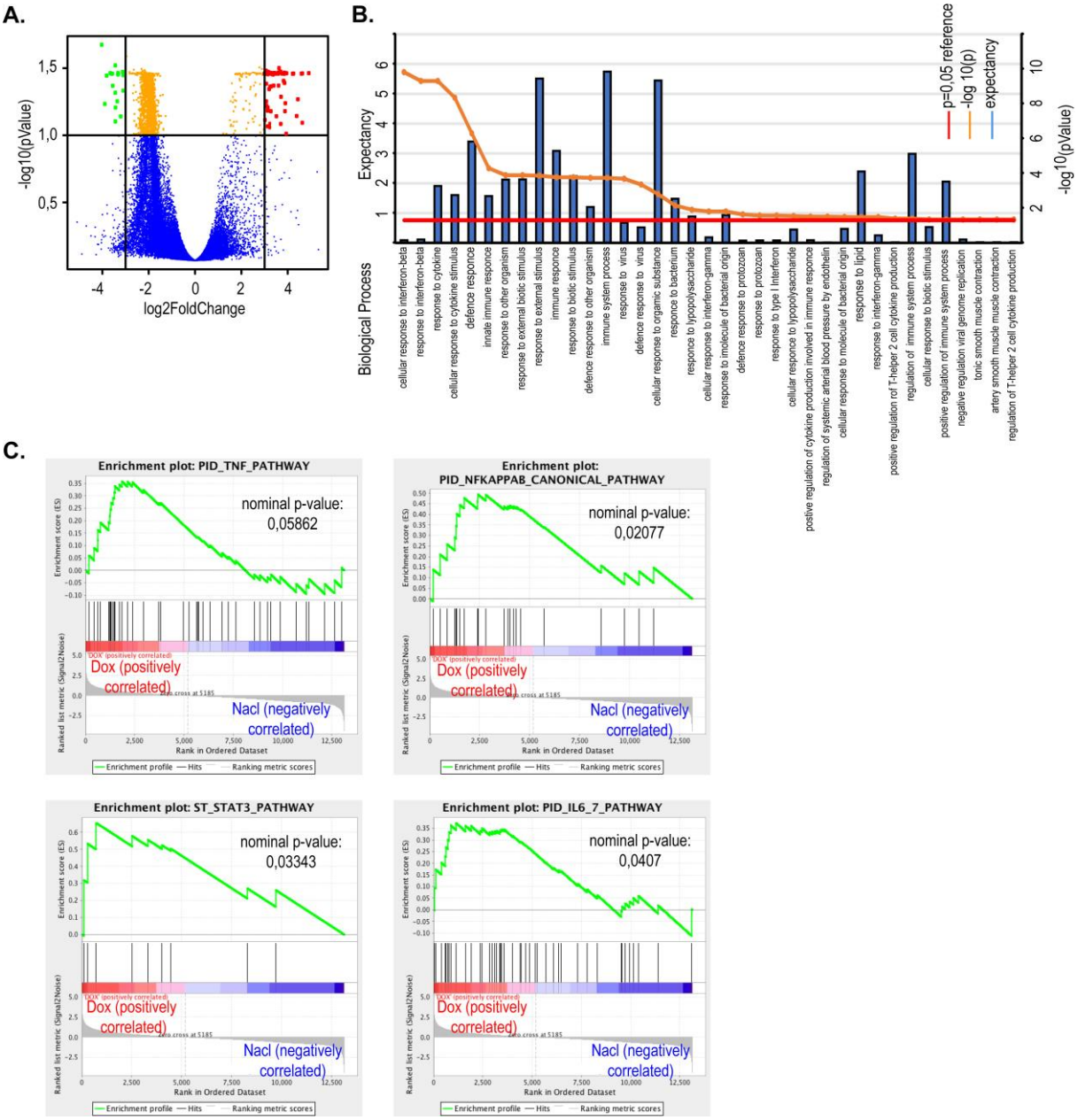

Supplemental Figure 6. (A) Volcano Plot for differential gene expression in the small intestine from *Tnk1*-knockin mice treated with doxycycline- vs saline-treated mice as a control (n=4/group). Scattered points represent genes: the x-axis shows the log2 fold-change of TNK1-expressing mice vs control mice, whereas the y-axis gives the -log10 p-value (shrinkage T-test, FDR correction). Red dots are thus genes significantly overexpressed in TNK1-expressing mice, whereas green dots are genes significantly under-regulated in TNK1-expressing mice **(B)** Gene ontology (biological processes) analysis of differentially expressed genes in the small intestine of TNK1-expressing mice. The horizontal axis represents the GO category, the vertical axis indicates the -log10 p-value of the tested GO category (Fisher's exact test, FDR correction). Greater -log10 p-value score correlates with increased statistical significance. **(C)** Gene Set Enrichment plots of differentially expressed genes belonging to TNFA pathway, NFkB-canonical-pathway, STAT3-pathway and IL6-pathway associated with TNK1 expression. The bar plot indicates the position of the genes on the expression data ranked by its association with TNK1 expression, i.e. red and blue colours indicate over- and under-expression in the mRNA.

Supplemental Figure 7

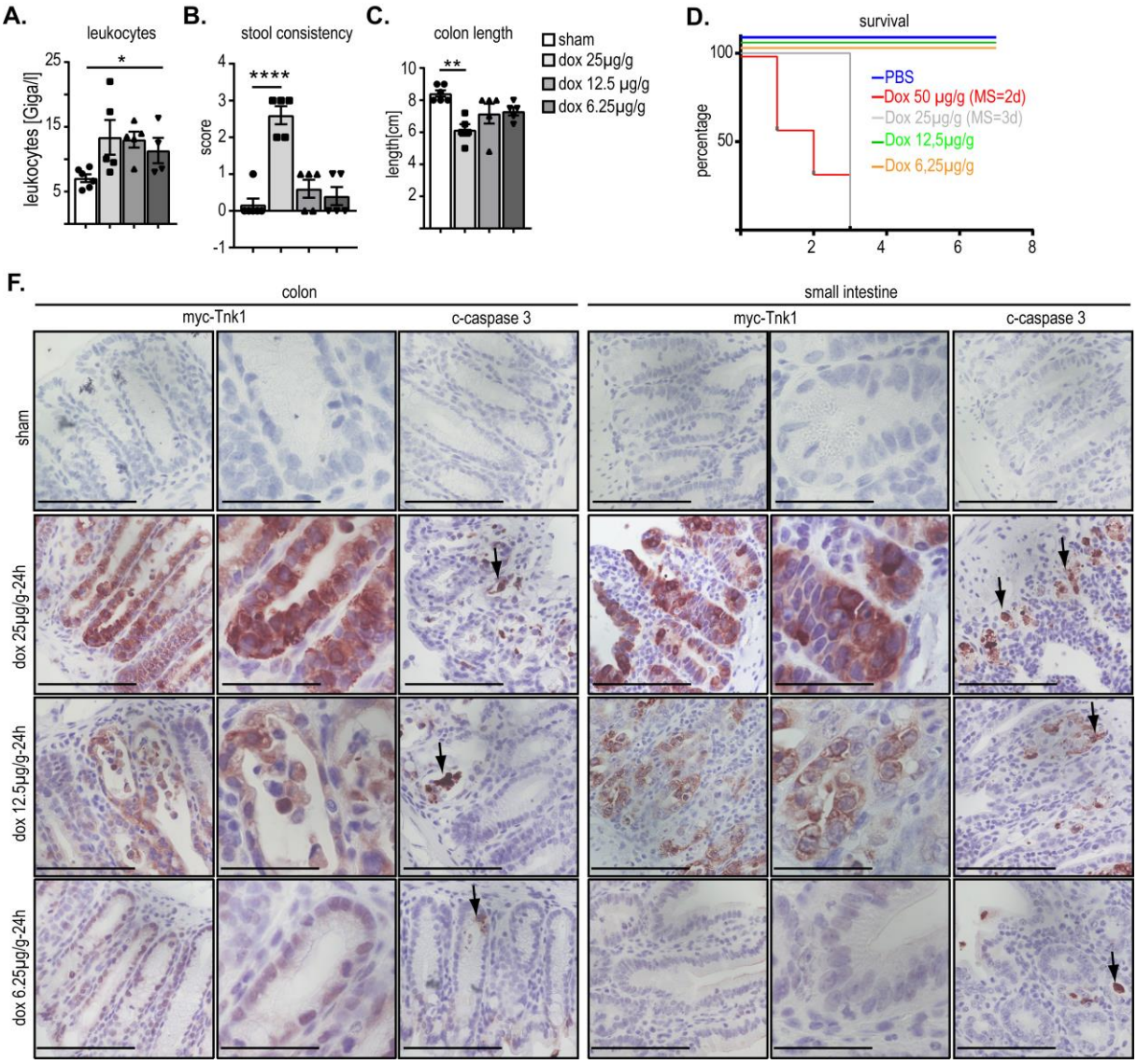

Supplemental Figure 7. Decreased TNK1 expression correlates with decreased intestinal apoptosis, improved clinical parameters and survival. Mice were treated with declining doses of doxycycline (25 µg/g; 12,5 µg/g and 6,25 µg/g) and analysed 24hrs upon administration. **(A)** Blood count analysis suggests inflammation (n=6/group, t=24h) as designated by an increase in the total number of white blood cells. **(B, C)** Graphs depict decrease in **(B)** stool score and **(C)** colon shrinking in mice with lower TNK1 expression (n=6/group). **(D)** Lower Doxycycline dosing and corresponding lower TNK1 expression improves animal survival. Kaplan-Meier survival analysis was performed. 50 µg/g doxycycline-treated mice are shown for the illustrative purpose. **(F)** Higher dose (25 µg/g) leads to high and uniform expression along the intestinal crypts. High TNK1 expression correlates with severe disruption of the mucosal architecture in small and large intestine associated with massive apoptosis and loss of goblet cells. Lower doxycycline dosing (12,5 µg/g and 6,25 µg/g) correlates with prominently lower TNK1 expression and resulting apoptosis. Representative images of the murine small and large intestine show immunoreactivity against myc-tagged TNK1 and apoptotic marker. Anova test was applied for multiple comparison analysis. The mean of each column was compared with the mean of a control column by Dunnett´s multiple comparison test. (*p≤0.05, **p<0.001, ***p<0. 0001). Scale Bar: 100µm.

Supplemental Figure 8

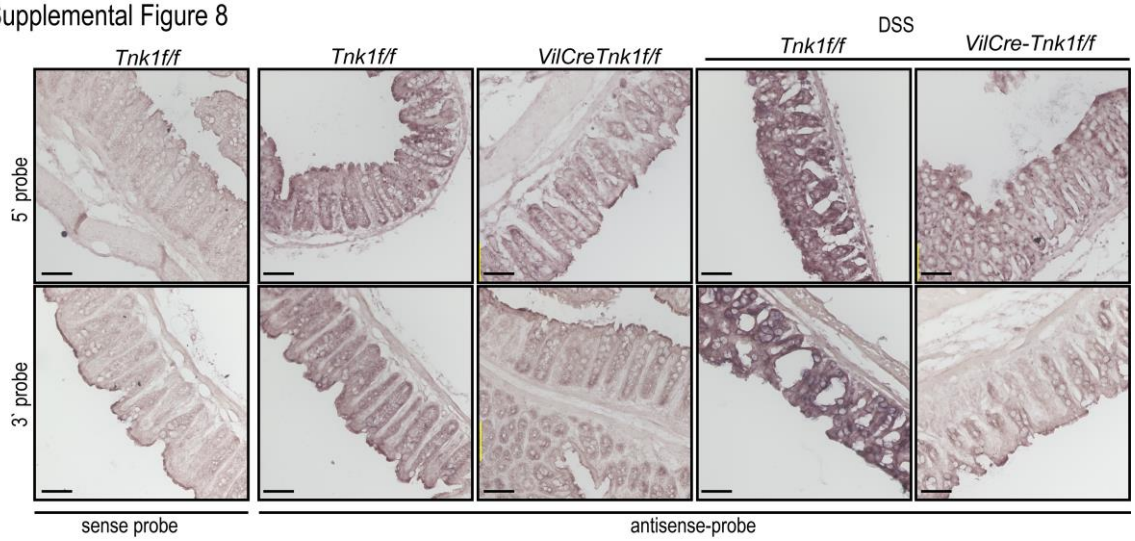

Supplemental Figure 8. In situ hybridisation was used to map *Tnk1* RNA in colon of wild-type (*Tnk1 f/f*) and intestine-specific-TNK1 knockout (*VilCreTnk1-/-)* mice fed with water or DSS. Representative image show basal level of *Tnk1* expression in colon of wild–type mice and its increase in response to an inflammatory insult. *Tnk1* expression was not detectable in the intestine-specific TNK1-knockout mice independently of DSS treatment. Identical results were obtained using two different probes (3´ and 5´binding probes). Three animals per group were analysed. Scale Bar: 100µl.

Supplemental Tables

Supplemental Table 1. Histological score in colitis

Score	Histological Changes
0	No evidence of inflammation
1	Low level of inflammation with scattered infiltrating mononuclear cells (1–2 foci)
2	Moderate inflammation with multiple foci
3	High level of inflammation with increased vascular density and marked wall thickening
4	Maximal severity of inflammation with transmural leukocyte infiltration and loss of goblet cells

Supplemental Table 2. Stool score

Score	Stool consistency	Blood
0	Normal Negative	
1	Soft but still formed	
2	Very soft	Blood traces in stool visible
3	Diarrhoea	Rectal bleeding

Supplemental Table 3. qRT-PCR primers

Gene	sequence 5`to 3`	sequence 5`to 3`	Company
murine Interleukin-6	gctaccaaactggatataatcagga	ccaggtagctatggtactccagaa	Biomers
murine TNF-alpha	tgggagtagacaaggtacaaccc	catcttctcaaaattcgagtgacaa	Biomers
murine TNK1	caagccgtgtttgtcttctgc	gaagggctgcttcaagaggt	Biomers
murine Lgr5	gactttaactggagcaaagatctca	cgagtaggttgtaagacaaatctagc	Biomers
murine Muc2	gctgacgagtggttggtgaatg	gatgaggtggcagacaggagac	Biomers
murine Gob-5	aggaaaaccccaagcagtg	gcaccgacgaacttgatttt	Biomers
murine TBP	caaacccagaattgttctcctt	atgtggtcttcctgaatccct	Biomers
murine Bax	tgaagacaggggccttttttg	aattcgccggagacactcg	Biomers
Gene	**Primer Name**	**Cat.No.**	**Company**
murine TNK1		PPM36921A-200	Qiagen
murineVilin		QT00172935	Qiagen
murine HMBS		QT00494130	Qiagen
murine Bcl2		QT00756282	Qiagen
murine XiaP		QT01755649	Qiagen
human TNK1		PPH143488-200	Qiagen
human HMBS		QT00014462	Qiagen
murineTNF	Mm_Tnf_1SG	QT00104006	Qiagen
murine Mcl1	Mm_Mcl1_1_SG	QT00107436	Qiagen
murine Bcl2-like 11 apoptosis facilitator		PPM03429F-200	Qiagen
murine Bcl2-antagonist/killer 1 (Bak1)		PPM03410F-200	Qiagen
murine BCL2-associated agonist of cell death (BAD)		PPM02916E	Qiagen
murine TBP	Mm_Tbp_1_SG	QT00198443	Qiagen

Supplemental Table 4. Antibodies for Western Blotting

Name	Company	Cat.-No.
Stat3 (79D7) Rabbit mAb	Cell Signaling Technology®	4904
Phospho-Stat3 (Tyr705)	Cell Signaling Technology®	9131
Myc-tag	Roche	11667149001
β-Actin	Sigma	A1978-200UL
Goat-anti-rabbit	Invitrogen	656120
Rabbit-anti-mouse	Invitrogen	816720
Cleaved-Caspase3	Cell Signaling Technology®	9661
Cleaved-Parp	Cell Signaling Technology®	9542
Stat1 Rabbit mAb	Cell Signaling Technology®	9172S
Phospho-Stat1 (Tyr701) (58D6) Rabbit mAb	Cell Signaling Technology®	9167
Stat1/2/3/5 Control Cell Extracts	Cell Signaling Technology®	9133S
Phospho-Stat5 (Tyr694) Rabbit	Cell Signaling Technology®	9351S
Stat5 (D2O6Y) Rabbit mAb	Cell Signaling Technology®	94205S
NF-κB p65 (D14E12) XP® Rabbit mAb	Cell Signaling Technology®	8242
Lamin B1 (D4Q4Z) Rabbit mAb	Cell Signaling Technology®	12586
Gapdh mAB	HyTestLtd	5G4 Mab6C5
TNK1 (C44F9) Rabbit mAb	Cell Signaling Technology®	4570
Phospho-TNK1 (Tyr277) (D46E7) Rabbit mAb	Cell Signaling Technology®	5638

Supplemental Table 5. Antibodies for Immunohistochemistry

Name	Company	Ref-No.
Stat3 (79D7) Rabbit mAb	Cell Signaling Technology®	4904
Phospho-Stat3 (Tyr705)	Cell Signaling Technology®	9131
TNK1 Polyclonal Antibody	Proteintech™	14199-1-AP
Myc-tag	Cell Signaling Technology®	2272S
Cleaved-Caspase3	Cell Signaling Technology®	9661
E-cadherin	BD Transduction	610182
Claudin-1	Abcam	ab15098

Supplemental material and methods

Polytrauma and Haemorrhagic Shock

For polytrauma (PT), haemorrhagic shock (HS) and caecal ligation and puncture (CLP), C57BL/6 mice aged 8-9 weeks (Jackson Laboratories, Bar Harbour, USA) with a mean body weight of 25 g (± 2.5 g) were used. Mice were anaesthetised with 2.5 % sevoflurane (Sevorane Abbott, Wiesbaden, Germany) in 97.5 % oxygen, in the course of polytrauma until euthanasia. For analgesia, 0.03 mg/kg of buprenorphine was administrated by subcutaneous injection. Polytrauma was induced by the application of blunt bilateral chest trauma, traumatic brain injury and a closed transverse femoral fracture as recently described in (2). After trauma induction, a catheter (Föhr Medical Instruments, Seeheim/Ober-Beerbach, and Germany) was inserted micro-surgically into the femoral artery, allowing the monitoring of mean arterial blood pressure (MAP) (blood pressure analyser, DSI, St. Paul, MN, USA) and controlled blood loss. A second catheter was inserted into the jugular vein, enabling fluid resuscitation and controlled infusion of catecholamines. For the induction of HS, mice were bled for 5-10 min to reach a mean blood pressure of 30 mmHg (± 5 mmHg), which was kept stable for 60 min. After haemorrhage, mice were resuscitated via the jugular vein with four times the volume of the drawn blood with a balanced electrolyte solution, administered over 30 min. During the 2h observation period after HS, anaesthesia and catecholamine support was adjusted in a standardised manner (0.01-0.12 µg/kg/min) to maintain a MAP of 50 mmHg. Four hours after polytrauma, blood was drawn by cardiac puncture. Plasma was obtained by centrifugation (5 min at 500 x g and 4°C) and stored at -80°C until further analysis. Sham animals underwent the same supportive treatment, including anaesthesia and catheterisation, without PT/HS. The porcine haemorrhagic shock was induced as previously described (3).

Caecal ligation and puncture (CLP)

For mouse lines used, anaesthesia and analgesia see above. The protocol was adapted from Rittirsch et al. 2009. After shaving and disinfecting the abdomen of the anaesthetised mouse, a 1.5-2 cm

incision was made longitudinally along the abdominal midline, stepwise dissecting the layers of the abdominal wall. The caecum was mobilised out of the abdominal cavity using a blunt forceps, leaving the remaining intestine internally. The caecum was then ligated with surgical suture in a central position, followed by perforation with a 21 G needle and extrusion of a small amount of faeces into the abdominal cavity. Afterwards, the caecum was relocated into the abdominal cavity. Wound closure was performed stepwise. Sham animals underwent the same treatment including anaesthesia and abdominal incision, but without ligation and puncture. Animals received postoperative fluid resuscitation by subcutaneous injection of 0,9% saline, 5 ml/100 g body weight), and were placed back in cages. Postoperative monitoring included checking and scoring for signs of distress and repeated buprenorphine injections every 6 hours (4).

Thromboelastometry measurement

Sodium citrate-anticoagulated venous whole blood was collected 24h after doxycycline or sham treatment for rotational thromboelastometry using a ROTEM® delta (Tem International GmbH, Munich, Germany). Coagulation was induced *via* the extrinsic pathway with (fibtem®) and without (extem®) inhibition of platelet activation to estimate platelet- and fibrin-dependent clotting. Parameters such as coagulation and clot formation time, alpha angle and (maximum) clot firmness were assessed for one hour.

Locomotor activity tracking

After injecting the animals with doxycycline (200µl, 50µg dox per gram of the mouse weight) or saline (200µl 0, 9%NaCl) solution (between 3 and 7 hours before the beginning of the dark phase), the home-cage locomotion of all animals was recorded during parts of the light phase and the dark phase (under red light conditions), starting 2.5 hours before the beginning of the dark phase. For the analysis, the software package EthoVision XT (Version 9, Noldus Information Technology, Wageningen, The Netherlands) was used.

Quantitative real-time PCR (qRT-PCR)

RNA was extracted from homogenised tissue with the RNeasy® Mini Kit (Qiagen) according to the manufacturer's instructions. cDNAs were prepared from 250 ng of total RNA, using the iScript™ cDNA Synthesis Kit (Biorad). PCR reactions were performed with iTaq™ Universal SYBR® Green Supermix reaction mixture (Biorad) according to the manufacturer's instructions. The thermal cycling conditions were comprised of 2min at 95°C, followed by 45 cycles of 15s at 95°C denaturation and 1min at 60°C anneal/extension. At least five animals per experimental group were analysed. The relative gene expression levels were calculated by "delta-delta Ct method" ($\Delta\Delta$Ct method). Primer sequences are listed in **Supplemental Table 3**.

Real-time PCR (TaqMan) for TNK1 expression in human samples was conducted following to the manufacturer's guidelines (Life Technologies) using a VIA VII Real-Time PCR System. Transcript abundances were calculated relative to beta-actin employing the standard-curve method. Differences experimental groups were determined using the Mann-Whitney U-test. Analysis of relative gene expression data using real-time quantitative PCR and the 2(-Delta Delta C(T)) Method (5).

Organoids preparation

Intestinal organoids were obtained from *VilCreTnk1-/-* mice and *Tnk1f/f* littermates as described previously (6, 7). Briefly, ileum was cut open longitudinal and washed in PBS. After scraping of intestinal villi, the ileum was cut into 2-3 mm pieces and washed in PBS for ten times. After incubation in 2 mM EDTA (Life Technologies) in PBS for 30 min on 4 °C, cells were passed through a 70 µm cell strainer while dissolved in 10 % FBS in PBS, and seeded into Matrigel (BD Biosciences, Heidelberg, Germany) with growth medium containing Advanced DMEM/F12 (Life technologies), 1x Glutamax (Life technologies), 1M HEPES (Life technologies), penicillin/streptomycin (Biochrom, Berlin, Germany), 1x N2 supplement (Life technologies), 1xB27 supplement (Life Technologies), 1.25 mM N-acetylcysteine (Sigma-Aldrich), 50 ng/µl EGF (Life Technologies), 20 % conditioned

supernatant containing noggin, and 10 % conditioned supernatant containing R-spondin. Organoids were grown for 10 days prior to further analysis.

Western blot

Tissue specimens were frozen and ground up in liquid nitrogen, and then lysed in for 10 min at 4°C in lysis buffer (10mM TRIS-HCl pH 7.6, 5mM EDTA pH 8, 50mM NACl, 50mM NAF, 1% Triton X-100, 0.2 mM NA3VO4, 10mM NA4P2O7, 1mM DTT, 1mM PMSF, 1X Protease Inhibitor Cocktail (Roche), 1X Phosphatase Inhibitor Cocktail (Roche)). Equal amounts of protein extracts (100µg) were fractionated by SDS-PAGE, transferred to nitrocellulose or PVDF membranes and sequentially probed with primary antibodies the appropriate primary antibody (see **Supplemental Table 4**). Protein was detected by enhanced chemiluminescence (ECL) bActin was used as a protein loading control to ensure equal loading.

STAT3 *in vitro* kinase assay

HEK293T cell were transfected with gfp-TNK1-wild-type (wt) or gfp-TNK1-K148R kinase dead (kd) expression plasmids. Cloning of TNK1 and generation of the TNK1-K148R mutant was done as previously described (8). Twenty-four hours after transfection cells were lysed and TNK1 immunoprecipitated using antibody against gfp-tag. Subsequently precipitated TNK1wt and TNK1kd proteins were used in cold kinase assay. Kinase reaction (50µl Kinase buffer (25mM TrispH7.5, 2mMDTT, 10mM MgCl2), 1µg recombinant STAT3 (Abcam #ab43618), 1µl ATP (10mM)) was incubated for 30 minutes on 37°C and subsequently terminated by addition of 3XSDS sample buffer. Samples were analysed by western blotting as described above by use of antibodies against STAT3, phosphor-STAT3 and GFP.

Histology and immunohistochemistry

Tissue samples were fixed in 4% paraformaldehyde and embedded in paraffin. For conventional histology, 3-5µm paraffin sections were stained with Harris haematoxylin and eosin (H&E). For

immunohistochemistry (IHC), sections were processed following standard immunostaining procedures with the primary and secondary antibodies listed in **Supplemental Table 5**. Sections were counterstained with 30% haematoxylin. Antigen retrieval was performed before incubation with primary antibodies.

Lung sections were analysed by an experienced pathologist blinded to the experimental groups for alveolar inflammatory cell (i.e. neutrophils, macrophages, and lymphocytes, respectively) infiltration, thickening of the alveolar membranes, protein debris in the airspaces, and alveolar oedema. These parameters were scored on a scale ranging from 0 (normal lung histology, 0.5 (minor histological injury), 1 (moderate and patchy histological injury), 1.5 (major histological injury < 25% of the lung involved), and 2 (major histological injury 25–50% of the lung involved). Scoring was done according to Matutte–Bello et al. 2011 (9). Hepatic activity index (HAI) for scoring of necroinflammatory activity in chronic hepatitis for applied to score and grade acute injury of liver tissue (10, 11). Pancreas sections were analysed for oedema, haemorrhages, parenchymal/fat necrosis and infiltration of polymorphonuclear leukocytes. The severity of colitis was estimated according to Wirtz et al., 2007 (12).

Semi-quantitative immunohistochemical quantification of TNK1 in Crohn´s disease

Bioptic material of six patients who underwent routine endoscopy and five patients with Chron's disease were stained with the monoclonal antibody TNK1 on paraffin section as described before. The samples were separated by tissue origin and Crohn's disease activity in four groups: healthy colon, healthy ileum, colon with active Crohn's disease, ileum with active Crohn's disease. Every group consisted of three different patients. Densiometric data of the stained epithelium was obtained at the microscope in an observation field with a magnification of x100 and the retrieved data used for further analysis. Data assembling was performed with CellProfiler 3.0.0 as described (13).

Blood and plasma

Blood obtained by cardiac puncture or from posterior vena cava was either used for differential blood screen (Scil VetABC haematology analyser) or placed in microtubes and spun down at 2000 rpm at 4°C for 10 min to obtain plasma. Plasma was stored at –80°C until analysis.

Measurement of cytokines, glucose and corticosterone

Interleukin 6 in serum was determined by sandwich enzyme-linked-immunosorbent assay technique (ELISA) according to manufacturer's recommendation. Levels below the detection limit of the assay were set to zero for statistical purpose. Corticosterone levels of the mice were determined in serum by using an Enzyme-Linked ImmunoSorbent Assay (ELISA, IBL International), according to the manufacturers' instructions. Blood glucose levels were determined with Accu-Chek® Aviva in (mmol/L).

RNA *in situ* hybridisation

Mouse colon tissue was fixed in ice-cold 4% PFA in PBS, embedded in PolyFreeze (Polysciences), and frozen section were prepared at 18 µm. RNA *in situ* hybridization was performed as described elsewhere (14). Two DIG-labeled RNA antisense probes were prepared targeting the 5' (primer pair: 5'-GCCTTCGCCAGTTCTCAGG-3' and 5'-GTTCCTCAAGGATGGGCCG-3') or 3' (5'-CGG AAC CTC AAG GTA GAC CA-3' and 5'-TGG GTG CCC CAT AGA GTT TA-3') region of mouse *TNK1* (NM_031880.3), respectively. Sense probes served as negative control for monitoring background signal. Antisense probe against mouse tyrosine hydroxylase (NM_009377.1) served as positive control (data not shown).

Gene expression analysis

Gene expression analysis was carried out using the SurePrint G3 Mouse Gene Expression 8x60K Microarray Kit (Design ID 028005; Agilent Technologies). Samples were labelled with the Low Input Quick Amp Labelling Kit (Agilent Technologies) according to the manufacturer's guidelines. Slides

were scanned using a G2565CA microarray scanner (Agilent Technologies). Expression data were extracted using the Feature Extraction software (Agilent Technologies). Pre-processing of expression data was performed according to Agilent's standard workflow. Using 5 quality flags (gIsPosAndSignif, gIsFeatNonUnifOL, gIsWellAboveBG, gIsSaturated, and gIsFeatPopnOL) from the Feature Extraction software output, probes were labelled as detected, not detected, or compromised. Gene expression levels were background corrected, and signals for duplicated probes were summarised by the geometric mean of non-compromised probes. After log2 transformation, a percentile shift normalisation at the 75% level was performed. Differentially expressed genes were calculated based on shrinkage-T statistic (false discovery rate < 0.1, absolute log2 fold-change > 3). All computations were performed using the R statistical software framework (http://www.R-project.org). Gene set enrichment analysis was calculated with GSEA software (http://software.broadinstitute.org/gsea/index.jsp). GEO accession numbers: GSE118023 (https://www.ncbi.nlm.nih.gov/geo/query/acc.cgi?acc=GSE118023).

Supplemental References

1. Chandrashekar, D.S., Bashel, B., Balasubramanya, S.A.H., Creighton, C.J., Ponce-Rodriguez, I., Chakravarthi, B., and Varambally, S. 2017. UALCAN: A Portal for Facilitating Tumor Subgroup Gene Expression and Survival Analyses. *Neoplasia* 19:649-658.
2. Martin, T., Moglich, A., Felix, I., Fortsch, C., Rittlinger, A., Palmer, A., Denk, S., Schneider, J., Notbohm, L., Vogel, M., et al. 2018. Rho-inhibiting C2IN-C3 fusion toxin inhibits chemotactic recruitment of human monocytes ex vivo and in mice in vivo. *Arch Toxicol* 92:323-336.
3. Knoller, E., Stenzel, T., Broeskamp, F., Hornung, R., Scheuerle, A., McCook, O., Wachter, U., Vogt, J.A., Matallo, J., Wepler, M., et al. 2016. Effects of Hyperoxia and Mild Therapeutic Hypothermia During Resuscitation From Porcine Hemorrhagic Shock. *Crit Care Med* 44:e264-277.
4. Rittirsch, D., Huber-Lang, M.S., Flierl, M.A., and Ward, P.A. 2009. Immunodesign of experimental sepsis by cecal ligation and puncture. *Nat Protoc* 4:31-36.
5. Livak, K.J., and Schmittgen, T.D. 2001. Analysis of relative gene expression data using real-time quantitative PCR and the 2(-Delta Delta C(T)) Method. *Methods* 25:402-408.
6. Peuker, K., Muff, S., Wang, J., Kunzel, S., Bosse, E., Zeissig, Y., Luzzi, G., Basic, M., Strigli, A., Ulbricht, A., et al. 2016. Epithelial calcineurin controls microbiota-dependent intestinal tumor development. *Nat Med* 22:506-515.
7. Sato, T., Vries, R.G., Snippert, H.J., van de Wetering, M., Barker, N., Stange, D.E., van Es, J.H., Abo, A., Kujala, P., Peters, P.J., et al. 2009. Single Lgr5 stem cells build crypt-villus structures in vitro without a mesenchymal niche. *Nature* 459:262-265.
8. Azoitei, N., Brey, A., Busch, T., Fulda, S., Adler, G., and Seufferlein, T. 2007. Thirty-eight-negative kinase 1 (TNK1) facilitates TNFalpha-induced apoptosis by blocking NF-kappaB activation. *Oncogene* 26:6536-6545.
9. Matute-Bello, G., Liles, W.C., Steinberg, K.P., Kiener, P.A., Mongovin, S., Chi, E.Y., Jonas, M., and Martin, T.R. 1999. Soluble Fas ligand induces epithelial cell apoptosis in humans with acute lung injury (ARDS). *J Immunol* 163:2217-2225.
10. Goodman, Z.D. 2007. Grading and staging systems for inflammation and fibrosis in chronic liver diseases. *J Hepatol* 47:598-607.
11. Ishak, K., Baptista, A., Bianchi, L., Callea, F., De Groote, J., Gudat, F., Denk, H., Desmet, V., Korb, G., MacSween, R.N., et al. 1995. Histological grading and staging of chronic hepatitis. *J Hepatol* 22:696-699.
12. Wirtz, S., Neufert, C., Weigmann, B., and Neurath, M.F. 2007. Chemically induced mouse models of intestinal inflammation. *Nat Protoc* 2:541-546.
13. Kamentsky, L., Jones, T.R., Fraser, A., Bray, M.A., Logan, D.J., Madden, K.L., Ljosa, V., Rueden, C., Eliceiri, K.W., and Carpenter, A.E. 2011. Improved structure, function and compatibility for CellProfiler: modular high-throughput image analysis software. *Bioinformatics* 27:1179-1180.
14. Wiegreffe, C., Simon, R., Peschkes, K., Kling, C., Strehle, M., Cheng, J., Srivatsa, S., Liu, P., Jenkins, N.A., Copeland, N.G., et al. 2015. Bcl11a (Ctip1) Controls Migration of Cortical Projection Neurons through Regulation of Sema3c. *Neuron* 87:311-325.